Journal of *Marine Science and Engineering*

MDPI

Article

Characterisation and Bioactivity Analysis of Peridinin-Chlorophyll *a*-Protein (PCP) Isolated from *Symbiodinium tridacnidorum* CS-73

Kanoknate M. Supasri [1], Manoj Kumar [1,*], Anna Segečová [1], Janice I. McCauley [1], Andrei Herdean [1], Matthew P. Padula [2], Tim O'Meara [3] and Peter J. Ralph [1]

1 Climate Change Cluster, Faculty of Science, University of Technology Sydney, Sydney, NSW 2007, Australia; Kanoknate.Supasri@student.uts.edu.au (K.M.S.); anna.segecova@gmail.com (A.S.); Janice.McCauley@uts.edu.au (J.I.M.); andrei.herdean@uts.edu.au (A.H.); peter.ralph@uts.edu.au (P.J.R.)
2 School of Life Sciences and Proteomics Core Facility, Faculty of Science, University of Technology Sydney, Sydney, NSW 2007, Australia; Matthew.Padula@uts.edu.au
3 Cytiva, Level 5, 7 Eden Park Drive, Macquarie Park, NSW 2113, Australia; tim.omeara@cytiva.com
* Correspondence: manoj.kumar@uts.edu.au

Abstract: Peridinin-Chlorophyll *a*-Proteins (PCP) are the major light harvesting proteins in photosynthetic dinoflagellates. PCP shows great variation in protein length, pigment ratio, sequence, and spectroscopic properties. PCP conjugates (PerCP) are widely used as fluorescent probes for cellular and tissue analysis in the biomedical field. PCP consists of a peridinin carotenoid; thereby, it can potentially be used as a bioactive compound in pharmaceutical applications. However, the biological activities of PCP are yet to be explored. In this study, we extracted, purified, and partially characterised the PCP from *Symbiodinium tridacnidorum* (CS-73) and explored its antioxidant, anti-cancer and anti-inflammation bioactivities. The PCP was purified using an ÄKTA™ PURE system and predicted to be of 17.3 kDa molecular weight (confirmed as a single band on SDS-PAGE) with an isoelectric point (pI) 5.6. LC-MS/MS and bioinformatic analysis of purified PCP digested with trypsin indicated it was 164 amino acids long with >90% sequence similarity to PCP of SymA3.s6014_g3 (belonging to clade A of *Symbiodinium* sp.) confirmed with 59 peptide combinations matched across its protein sequence. The spectroscopic properties of purified PCP showed a slight shift in absorption and emission spectra to previously documented analysis in *Symbiodinium* species possibly due to variation in amino acid sequences that interact with chl *a* and peridinin. Purified PCP consisted of a 19-amino-acid-long signal peptide at its N terminal and nine helixes in its secondary structure, with several protein binding sites and no DNA/RNA binding site. Furthermore, purified PCP exhibited antioxidant and in vitro anti-inflammation bioactivities, and anti-cancer activities against human metastatic breast adenocarcinoma (MDA-MB-231) and human colorectal (HTC-15) cancer cell lines. Together, all these findings present PCP as a promising candidate for continued investigations for pharmaceutical applications to cure chronic diseases, apart from its existing application as a fluorescent-probe.

Keywords: *Symbiodinium*; Peridinin-Chlorophyll *a*-Proteins (PCP); bioactivity; antioxidant; anti-cancer; anti-inflammation

Citation: Supasri, K.M.; Kumar, M.; Segečová, A.; McCauley, J.I.; Herdean, A.; Padula, M.P.; O'Meara, T.; Ralph, P.J. Characterisation and Bioactivity Analysis of Peridinin-Chlorophyll *a*-Protein (PCP) Isolated from *Symbiodinium tridacnidorum* CS-73. *J. Mar. Sci. Eng.* **2021**, *9*, 1387. https://doi.org/10.3390/jmse9121387

Academic Editors: Angela Sardo and Giovanna Romano

Received: 9 October 2021
Accepted: 2 December 2021
Published: 6 December 2021

1. Introduction

Peridinin-Chlorophyll *a*-Protein (PCP) is a water-soluble light harvesting complex (LHC) protein in photosynthetic dinoflagellates [1]. PCP also protects cellular photosynthetic machinery from photodamage by scavenging free radicals and quenching singlet oxygen during heat stress [1,2]. Therefore, reduced levels of PCP in thermally sensitive *Symbiodinium* dinoflagellates exposed to thermal stress is possibly linked to coral bleaching [3]. Apart from photoprotection and light harvesting roles, PCP conjugated with antibodies,

proteins and peptides is also used commercially for fluorescent immunolabelling in medical research for fluorescent activated cell sorting (FACS). For example, Peridinin Chlorophyll Protein-Cyanin5.5 (PerCP-Cyanin5.5) and PerCP-vivo700-based PCP tandem conjugates are commercially available with a range of antibodies to label human cells [4]. The PCP complex has recently been used to probe plasmonic interactions in various nanostructures such as functionalised silver nanowires for real-time bioconjugation sensing [4–6].

Carotenoids and chlorophyll are among the most abundant natural pigments in nature. In particular, marine carotenoids such as fucoxanthin have shown potential in improving human health, and have therefore received much attention as pharmaceuticals and nutraceuticals [7–9]. Dinoflagellates represent a potential source of peridinin carotenoids in the form of PCP, which has a structure similar to that of fucoxanthin; however, its biological activities have not been explored sufficiently. Peridinin from the dinoflagellate have been demonstrated to induce apoptosis in cancer cells [10], and to inhibit eosinophil cell-mediated allergic response in mice [11].

PCP in dinoflagellates shows great variation in amino acid sequences and spectroscopic properties [12,13], and can be classified in to two types—a homodimer of 15 kDa monomeric units and a monomer of 32–35 kDa molecular mass [14,15]. Exceptionally, the dinoflagellate *Amphidinium carterae* possesses a trimeric PCP complex, which is formed by three copies of the monomeric PCP [16]. However, this trimeric PCP may not necessarily function as a light-harvesting complex [13]. Genomic and transcript analysis of PCP genes in various dinoflagellates has revealed that PCP genes are nuclear-encoded, intron-less, and exist in tandem arrays [12,13]. Therefore, PCP gene heterogeneity is believed to be the source of multiple PCP isoforms in dinoflagellates with large variation in isoelectric point (pI) values [12].

PCP characterisation in dinoflagellates has largely focused on determining spectroscopic properties and photosynthetic energy transfer analysis. The bioactive potential of PCP as an antioxidant, anti-inflammatory and anti-cancer agent remains to be explored. Although *Symbiodinium* LHCs are of considerable significance, the molecular level understanding of these protein–pigment complexes are limited compared to that of their counterparts in higher plants, green algae, diatoms and photosynthetic bacteria. Recently, we reported the molecular mechanism of PCP accumulation in *Symbiodinium* under low light conditions, which can be used as a strategy to scale up its production for industrial purpose [17]. Therefore, it is imperative to purify and characterise PCP from *Symbiodinium* sp., which exhibits multiple forms of PCP, exploring its biological activities to enhance its pharmaceutical applications as marine bio-products. This study describes the extraction and purification of PCP from the marine dinoflagellate *Symbiodinium tridacnidorum* (ITS2-type A3, CS-73) using the ÄKTA™ PURE system. The spectroscopic properties of purified PCP and the amino acid sequence of purified PCP was then determined using mass spectrometry, along with bioinformatic analysis to predict its structure and functional domains. Furthermore, the bioactivities of the purified PCP including antioxidant, cytotoxicity, and anti-inflammation were examined to explore its potential use in pharmaceutical applications.

2. Materials and Methods

2.1. Algal Culture

Our previous studies showed a slow growth, but higher photosynthetic performance and a 4-fold accumulation of PCP in *S. tridacnidorum* (ITS2-type A3, CS73) cultures when grown under low light intensity of 30 µmol photons m^{-2} s^{-1} for three weeks [17]. Therefore, for PCP extraction, *S. tridacnidorum* cultures obtained from the UTS algal culture repository were grown in 100 mL of Daigo's IMK media (2.56 g/L artificial seawater) (Nihon Pharmaceutical Co., Ltd., Tokyo, Japan) under a white fluorescent lamp at an intensity of 30 µmol photons m^{-2} s^{-1} within a climate-controlled incubator at 25 °C under 12:12 h light and dark conditions as described previously [17]. The algal cultures (three biologi-

cal replicates) were harvested in the late exponential phase and used for PCP extraction, purification, and bioactivity analysis.

2.2. Extraction and Isolation of PCP

A PCP extraction procedure was performed according to Ogata et al. [18] with minor modifications. Briefly, *Symbiodinium* cultures were harvested by centrifugation at 8000× *g* for 10 min at 4 °C. An algal pellet was re-suspended in 50 mM Tris-HCl buffer pH 7.5 and cell lysis was performed using an ultra-sonication probe (Q55 Sonicator, Thomas Scientific, Swedesboro, NJ, USA) with cycles lasting 25 s, repeated 5 times with 25 s off-time between each sonication cycle, while remaining on ice to avoid excess heating during sonication. The resulting lysate was centrifuged at 15,000× *g* for 15 min at 4 °C to remove the cell debris and unbroken cells. Ammonium sulphate salt was added into the resulting supernatant at 50% saturation to precipitate PCP overnight at 4 °C, followed by centrifugation at 8000× *g* for 10 min at 4 °C. The orange-coloured supernatant containing the water-soluble PCP was desalted using Sephadex G-25 in a PD-10 desalting column and later concentrated using 10 kDa centrifugal filters (Amicon® Ultra, Merck, Bayswater, VIC, Australia). The resulting PCP was passed through a HiTrap® Q HP column using ÄKTA™ PURE system and the fractions were eluted by 20 mM Tris-HCl (pH 8.0) with a linear gradient of NaCl from 0–0.5 M in the same buffer. The deep orange coloured fraction containing the water-soluble PCP was collected and stored at −20 °C in complete darkness for further use.

2.3. Sodium Dodecyl Sulphate-Polyacrylamide Gel Electrophoresis (SDS-PAGE)

SDS-PAGE was used to analyse *Symbiodinium* PCP under denaturing conditions. The purified PCP was diluted with a 2× Laemmli sample buffer (4% (*w*/*v*) SDS, 0.2% (*w*/*v*) bromophenol blue, 20% (*v*/*v*) glycerol, 200 mM DTT) and 5% (*v*/*v*) β-mercaptoethanol. The PCP was separated using an electrophoresis system (Bio-Rad Mini-PROTEIN®) in 5–12% TGX Stain-Free™ Precast Gels. The protein was separated using a tri-glycerol-SDS (TGS) electrophoresis buffer and stained with Coomassie brilliant blue R-250 according to Jiang et al. [12].

2.4. Protein Digestion and LCMS/MS Analysis

2.4.1. Protein Digestion and Peptide Recovery

The Coomassie blue-stained band of purified PCP was excised from the gel and in-gel digested with trypsin. The band was excised and chopped into small pieces and de-stained in 200 µL of 1:1 acetonitrile (ACN) and 100 mM ammonium bicarbonate solution at room temperature for 10 min. De-stained gel pieces were dehydrated with 200 µL of 100% ACN at room temperature for 10 min. Trypsin (15 ng/µL) digestive enzyme in 100 mM ammonium bicarbonate was added to the gel piece and the enzymatic reaction was performed overnight at 37 °C in an incubator. Later, digested peptides were extracted twice using an extraction solvent (50 µL of acetonitrile/2% formic acid) for 10 min in a digitally controlled ultrasonic water bath. The extracted peptide solution was dried in a vacuum concentrator (SpeedVac DNA120) until it reached 10 µL volume. The peptide solution was centrifuged at 14,000× *g* for 10 min to remove any insoluble material prior to LC/MS/MS analysis.

2.4.2. LCMS/MS Analysis of Peptides

Trypsin-digested peptides were analysed by LC-MS/MS according to Supasri et al. [17]. Peptide solution (20 µL) was loaded at 15 µL/min onto a nanoEase C18 trapping column (Waters, Milford, MA, USA) with 2% acetonitrile and 0.1% formic acid for 3 min. The peptides were eluted from the trapping column onto a PicoFrit column (75 µm ID × 250 mm; New Objective, Woburn, MA, USA) packed with C18AQ resin (3 µm; Michrom Bioresources, Auburn, CA, USA). Repeated injections of standard samples (six bovine tryptic digest equal molar mix, New England Biolabs, Ipswich, MA, USA) were used to monitor the instrument stability. Peptides were eluted from the column and into the source of a mass

spectrometer (Q Exactive Plus, Thermo Scientific, Scoresby, Australia) using the following program: 5–30% MS buffer B (98% acetonitrile + 0.2% formic acid) over 90 min, 30–80% MS buffer B over 3 min, 80% MS buffer B for 2 min, 80–5% for 3 min. The eluting peptides were ionised at 2000 V. A data-dependent MS/MS (dd-MS2) experiment was performed, with a survey scan of 350–1500 Da performed at 70,000 resolutions for peptides of charge state 2+ or higher with an automatic gain control (AGC) target of 3×10^6 and maximum injection time of 50 ms. The top 12 peptides with high AGC value were fragmented in the higher-energy collisional dissociation (HCD) cell using an isolation window of 1.4 m/z and an AGC target of 1×105 and maximum injection time of 100 ms. Fragments were scanned in the Orbitrap analyser at 17,500 resolution and the product ion fragment masses measured over a mass range of 100–2000 Da. The mass of the precursor peptide was then excluded for 30 s.

Raw MS files from each digest analysis were searched using PEAKS Studio v8.5 (Bioinformatics Solutions, Waterloo, ON, USA) against a customised proteomic database that combine the proteomic datasets of *Symbiodinium microadriacticum* downloaded from Uniprot (https://www.uniprot.org/proteomes/UP000186817, accessed on 15 January 2021) and proteomic datasets for Symbiodiniaceae algae including *Fugacium kawagutii*, *Breviolum minutum*, *Symbiodinium* sp. and *Cladocopium* sp. (http://sampgr.org.cn/, accessed on 15 January 2021) [19] for protein identification. The search parameters were set as follows: tolerance of one missed cleavage of trypsin, oxidation (M) for methionine as the variable modifications, and carbamidomethyl (C) for cysteine as fixed modifications. Three missed cleavage sites were allowed, with a parent and fragment mass error tolerance of 20 ppm and 0.1 Da, respectively. The charge states of peptides were set to +2 and +3. The threshold selection for random protein sequences was a PEAKS probability-based ion score greater than 15 and false-discovery rate of 0.1%. Automated variance stabilisation, normalisation, isotopic correction and median correction were selected as pre-setting parameters in PEAKS Studio v8.5 software. A protein with at least one unique peptide was considered for protein identification and for protein quantification and regulation analysis. Peptides were further validated by manual inspection of the MS/MS spectra for the peptide to ensure the b- and y-ion series were sufficiently extensive for an accurate identification.

2.5. Bioinformatics Analysis of Purified PCP

The theoretical isoelectric point and molecular weight of the purified PCP protein that matched with high confidence to PCP amino acid sequence of SymA3.s6014_g3 (belonging to clade A of *Symbiodinium* sp.) were predicted by ExPaSy PeptideMass (https://web.expasy.org/peptide_mass/, accessed on 24 January 2021). The signal peptide analysis was conducted by Phobius software (https://phobius.sbc.su.se/, accessed on 25 January 2021). Furthermore, several bioinformatic tools including QUARK, COACH and I-TASSER were used to predict the 3-dimensional structure of protein molecules from the amino acid sequence, and to deduce their biological function based on the sequence-to-structure-to-function. Furthermore, PredictProtein was used to predict secondary structure, solvent accessibility, transmembrane helices and globular regions (https://predictprotein.org/, accessed on 26 January 2021).

2.6. PCP Spectroscopic Properties Analysis

The absorption spectra and fluorescence emission spectra were also investigated using microplate spectrophotometers (Tecan Infinite M1000 PRO, Tecan Group Ltd., Männedrof, Switzerland). The absorption spectra were measured across the range 400–800 nm with a 2 nm wavelength step size at room temperature. The fluorescence emission spectra were excited at 480 nm and measured from 550 to 800 nm.

2.7. Bioactivity Assays

2.7.1. ABTS Radical Scavenging Assay

Free radical scavenging activity of PCP was determined by 2,2′-azino-bis3-ethylbenzthaioline-6-sulfonic (ABTS) radical cation decolourisation assay according to Re et al. [20]. ABTS n radical was produced by the reaction between 7 mM ABTS radical in water and 2.45 mM potassium persulfate (1:1), stored in the dark at room temperature for 12–16 h before use. ABTS radical solution was then diluted with methanol to obtain an absorbance of 0.700 at 734 nm. After the addition of 5 µL of PCP (concentration ranged from 0.2–1.4 mg/mL) to 4 mL of diluted ABTS radical solution, the absorbance was measured 30 min after initial mixing. An appropriate solvent blank was run in each assay. All of the measurements were carried out at least three times. Ascorbic acid was used as a standard. Percentage inhibition of absorbance at 734 nm was calculated by the following equation:

$$\%inhibition = \left[\frac{A0 - A1}{A0}\right] \times 100$$

$A0$ expresses the control; $A1$ expresses the absorbance of the purified PCP.

2.7.2. Anti-Tumour and Anti-Inflammation Assay

Cell Culture Preparations

Various cells including Abelson murine leukaemia virus-induced tumour macrophage (RAW 264.7), human metastatic breast adenocarcinoma (MDA-MB-231) and human colorectal (HTC-116) cancer cell lines were prepared as described previously [21]. Briefly, cell lines were cultured in RPMI 1640 medium supplemented with 10% (v/v) foetal bovine serum (FBS), L-glutamine and incubated in a humidified incubator at 37 °C in a 5% CO_2 atmosphere. Cells were treated with purified PCP dissolved in dimethyl sulfoxide (DMSO), added to the culture medium at a concentration ranged 12.5–400 µg/mL and incubated for 24 h. The concentration of DMSO in PCP applied to cells did not exceed 1% (v/v).

Anti-Tumour Assay

Anti-tumour activity of PCP was determined based on cytotoxicity using 3-(4,5-dimethylthiazol-2-yl)-5-(3-carboxymethoxyphenyl)-2-(4-sulfophenyl)2H-tetrazolium) (MTS) colorimetric assay according to previous studies [21]. Cells (HTC 116; MDA-MD 231 and RAW 264.7) were seeded (25,000 cells/well) in a 96-well plate and kept at 37 °C and 5% CO_2. After 24 h, cell lines were treated with purified PCP (12.5–400 µg/mL) followed by incubation at 37 °C and 5% CO_2. After 24 h, 10 µL of MTS reagent was added into each well and incubated for 2 h. Finally, the absorbance at 490 nm was read using a microplate reader. The percent cytotoxicity of various concentrations of purified PCP was calculated against positive growth control (1% DMSO) and negative growth control (10% DMSO). The percent cytotoxicity was plotted as a function of purified PCP concentration to illustrate its anti-tumour potential.

Anti-Inflammatory Activity

RAW 264.7 macrophage cells were used to test the anti-inflammatory potential of PCP protein. RAW cells stimulated with lipopolysaccharide (LPS) derived from *Escherichia coli* was used to induce nitric oxide (NO) synthesis [21,22]. The cells were seeded (25,000 cells/well) in 96-well plates and incubated at 37 °C and 5% CO_2. When the cells were fully adhered after 24 h, they were treated with various concentrations of purified PCP (12.5–400 µg/mL) reconstituted in DMSO and 1 µg/mL LPS for 24 h. Finally, an aliquot of the conditioned medium was mixed with an equal volume of Griess reagent (1% sulphanilamide and 0.1% N-(1-naphthyl) ethylenediamine dihydrochloride solution). After 10 min incubation at room temperature, the absorbance was determined at 540 nm. Sodium nitrite, diluted to concentrations of 0–100 µM, was used to generate a standard curve. Data was expressed as a percentage of nitrite production compared to positive (1% DMSO) and negative growth controls (10% DMSO) [23].

2.8. Statistical Analysis

All assays were performed in triplicate and the data are expressed as mean ± standard deviation (SD; n = 3). Data were analysed by one-way analysis of variance (ANOVA) with Turkey's multiple comparisons to determine significant differences of mean values using GraphPad Prism version 8.00 (GraphPad Software, San Diego, CA, USA).

3. Results and Discussion

3.1. PCP Extraction, Purification, pI and Protein Sequence Analysis

Our previous studies showed PCP accumulation under low light condition (30 µmol photons m^{-2} s^{-1}) in *S. tridacnidorum* cultures [17]. Therefore, algal cultures grown under low light conditions were harvested in their late exponential phase. Subsequently, PCP extraction and purification using the AKTA™ PURE (Figure 1A) was successfully achieved with a yield of 10.2 mg/g dry algae weight after ammonium salt precipitation and desalting processed through an intuitive ion-exchange chromatography ÄKTA™ PURE system. A highly purified PCP protein with an absorbance peak at 484 nm was eluted as a clarified deep-orange solution (Supplementary Figure S1).

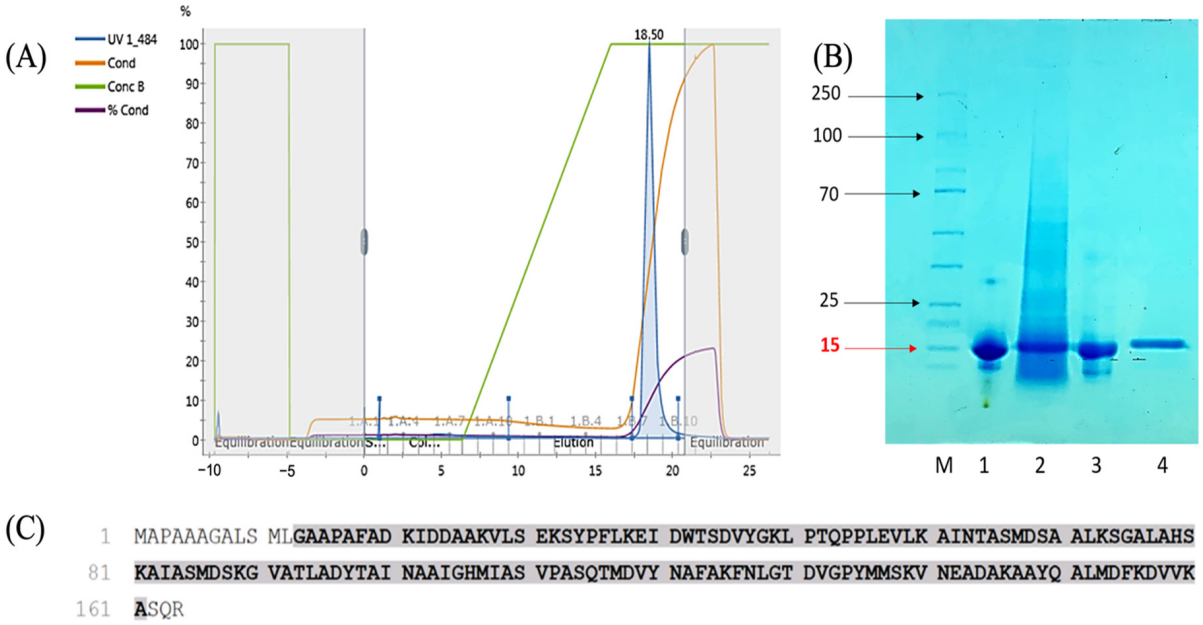

Figure 1. Chromatogram of *S. tridacnidorum* purified PCP using ÄKTA™ PURE system (**A**). SDS-PAGE analysis of PCP extracted from *S. tridacnidorum* (**B**). Lane M represent marker proteins, PCP commercial standard (**lane 1**), crude PCP (**lane 2**), desalted PCP (**lane 3**) and a single band of purified PCP with ÄKTA™ PURE system (**lane 4**). PCP sequence matched to accession SimA3.s6014_g3 (*Symbiodinium* clade A) using PEAKS 8.5 software (**C**). Shaded amino acid sequence denotes identified peptides and sequence coverage of trypsin-based PCP digestion.

The purity of the PCP was examined by SDS-PAGE (Figure 1B), which resolved the PCP into a single band of molecular weight (MW) between 15 and 20 kDa, which was determined theoretically to be 17.3 kDa based on protein sequence coverage. PCP in dinoflagellates occur mainly in two different forms, a short form with each monomeric unit having a mass of 14–16 kDa (homodimeric form) and a long form with a mass of 30–35 kDa (monomeric form), possibly due to gene duplication. Exceptionally, *A. carterae* [24] and *Symbiodinium* sp. (CS-156) [12,13] exhibited three monomeric PCP assembled into a trimeric complex. In present study, SDS-PAGE analysis suggested the possible occurrence of a short form of PCP in *S. tridacnidorum* with a monomeric unit of molecular mass of ~15–20 kDa. The occurrence of such monomeric units in a homodimeric PCP has been suggested to be similar in amino acid sequence and configuration [25]. Similar to our findings, Weis et al. [15] identified a short form of PCP in *S. muscatinei*, a symbiotic dinoflagellate

resident in the sea anemone *Anthopleura elegantissima*. However, in *Symbiodinium* sp. (CS-156), a monomeric PCP of Mw 32.7 kDa was identified [12]. Both monomeric and homodimeric PCP have been detected in *S. microadriaticum*, while *S. kawagutii* and *S. pilosum* possessed only a single form of PCP; monomeric and homodimeric forms, respectively [26]. Compared to water-soluble PCP, thylakoid intrinsic chlorophyll a/c2-peridinin-protein complexes (acpPC) of 18–20 kDa have also shown abundance in *Symbiodinium* cells with their N-terminal region, similar to the LHCs of higher plants. Jiang et al. [13] highlighted the existence of a functional trimeric acpPC (Mw—18.3 kDa of each monomeric unit) in *Symbiodinium* sp. (CS-156). However, PCP identified in this study did not match with acpPC sequence, thus excluded its existence as acpPC.

Purified PCP resolved as a single band by SDS-PAGE was excised and digested with trypsin enzymes to determine PCP amino acid sequence. Trypsin, being a serine protease, cuts PCP protein at the carboxyl side of arginine and lysine residues, resulting in smaller peptides (700–1500 Da), which are ideal for LCMS analysis. Trypsin-based digestion of PCP and subsequent MS analysis identified a total of 59 peptides with two unique peptides and a peptide score −10lgP value > 220) that covered >91% of protein sequence matched to accession SimA3.s6014_g3 (*Symbiodinium* clade A) (Supplementary Figure S2A,B). Earlier, Jiang et al. [12] and Jiang et al. [13] also performed the trypsin-based digestion for PCP sequence analysis in *Symbiodinium* sp. (CS-156) and concluded the occurrence of monomeric PCP (Mw 32.7 kDa) and a trimeric PCP (apcPC; Mw 18.3 kDa of each subunit).

The bioinformatic analysis of PCP sequence inferred from Figure 1C identified 164 amino acids with theoretical Mw 17.13 kDa and isoelectric point (pI) 5.60. Regardless of PCP size that an individual dinoflagellate species expresses, multiple PCP isoforms with distinct pIs have been observed in various dinoflagellates. Most isoforms from *A. carterae*, *Glenodinium* (*Heterocapsa*) sp. and *S. microadriaticum* exhibited a basic pI 7.2–7.7 [12,27,28]. However, several symbiotic dinoflagellates produced predominantly acidic PCP isoforms with pI ranges similar to the predicted in the present study, including *S. goreauii* [29], *Symbiodinium* from *Montastrea annularis*, and *M. cavernosa* [30]. In addition, the calculated pI values of PCP in *G. polyedra* and *Symbiodinium* from *A. formosa* were registered as 6.28 and 5.28, respectively. Furthermore, differences in spectroscopic properties of isoforms between inter- and intra- species has also been observed [26,27,31]. However, whether PCP isoform variation is due to post-translational modification, protein degradation, or genetics remains unclear. The nuclear genes that encode PCP are identified as intronless and exist in multigene families set in tandem arrays [32]. Evidence is mounting to suggest that the expression of distinct PCP isoforms is primarily due to genetic diversity among gene copies in PCP arrays [25,32,33]. The functional significance of PCP isoform diversity is suggested to help algae in harvesting photonic energy more efficiently, while adapting to a variety of habitats with low light intensities and poor nutrient [34].

The identified PCP protein sequence inferred from Figure 1C appeared to contain a signal peptide of 19 amino acids. This signal peptide comprised of (i) a hydrophilic and a positively charged n-region (1–3 amino acids), (ii) a central hydrophobic h-region at 4–14 residues, and (iii) a c-region from 15 to 19 amino acids with the cleavage site for signal peptidase (SPase) followed by a long non-cytoplasmic protein sequence region (from 20 to 164 amino acids) (Supplementary Figure S3A). The comparison of the translated PCP sequences with peptide sequencing using LC–MS/MS, revealed that the mature protein starts at Asp53 (D). Protein sequence alignment of *F. kawagutii* V1, V2 and V3; *S. microadriacticum*, *C. goreaui*, Symbiodiniaceae clade C, Symbiodiniaceae clade A, and *B. minutum* PCP; and the identified sequence in this study showed that all mature PCP begin at Asp53, and most of them share a sequence of DKIDDAAK at the N terminus [12,19]. Additionally, the hydrophobic h-region of the signal peptide (SP) was found to be rich in A (Alanine) residues (predicted by ExPASy ProtScale tool) similar to other Symbiodiniaceae family PCP (Supplementary Figure S3B), which is a common feature of various SPs of nuclear encoded thylakoid proteins [35]. This SP sequence analysis is in agreement with co-crystallisation of PCP and digalactosyl diacyl glycerol (DGDG) [36], which is mostly

found in the inner thylakoid membrane [12], supporting that PCP is located in the thylakoid lumen [12,13,36].

3.2. Secondary Structures, Topology and Protein Binding Features of PCP Protein Sequence

We further characterised the PCP sequence using diverse protein structure bioinformatic tools to predict its secondary structure and other features. Protein prediction tools provided in-depth information about its secondary structure, solvent accessibility, topology features and protein/DNA/RNA bindings domains (Supplementary Figure S4A). Interestingly, a 164-amino-acid-long PCP sequence possessed 11 helixes that covered >56% of the structure and 45% of the random coiled structures with 55% of exposed and 39% buried structural domains (Supplementary Figure S4B,C). Furthermore, based on the degree of flexible and rigid residues in the protein sequence, the identified PCP was suggested to have an intermediate level of flexibility/rigidity with most of residues (>80%) appeared in PROFbval (35–70) and only 10% each in the score value of <30 and >70. Furthermore, the PCP protein sequence was found to have only protein binding domains (scoring RI value 0–35 with >70%) with zero DNA/RNA binding domains (Supplementary Figure S4A).

The flexibility of residues is strongly correlated with secondary structures and solvent accessibility [37]. A regular secondary structural element such as alpha helices and beta strands tend to be more stable than random coils. Buried segments tend to be less flexible than exposed ones. Consequently, this analysis suggested that the identified PCP is a more flexible and stable protein [38]. Furthermore, understanding of the protein binding residues allows structure-based drug design. Drug molecules usually affect the interaction between the target protein and its normal ligand [37]. However, fewer than 0.36% of all proteins of known sequence in UniProt correspond to a known experimental 3D structure in the Protein Data Bank (PDB) [39]. Therefore, it is essential to use computational tools to reliably and rapidly identify protein-, DNA- and RNA-binding proteins or residues. Our analysis of the protein binding capacity of PCP with no DNA/RNA binding domains, supports its suitability in designing diverse protein-conjugates including PerCP/Cyanine5.5 Streptavidin and PerCP-eFluor 710 for indirect immune-fluorescent staining as used in biotechnology applications [40].

Furthermore, we explored I-TASSER and COACH to predict a 3D model of predicted PCP protein sequence (Figure 2A,B). I-TASSER (Iterative Threading ASSEmbly Refinement) is a hierarchical approach to protein structure prediction and structure-based function annotation. To predict the 3D model of the PCP protein in the present study, we first identified structural templates from the Protein Data Bank (PDB) by the multiple threading approach LOMETS, with full-length atomic models constructed by iterative template-based fragment assembly simulations. I-TASSER only uses the templates of the highest significance in the threading alignments, the significance of which are measured by the Z-score.

Based on this analysis, the predicted PCP sequence matched close to 1 pprM PCP template of *A. carterae* from RCSB PDB (protein databank; https://www.rcsb.org/structure/1ppr, accessed on 26 January 2021) with a Z-score 2.8, C-score 1 and TM score 0.75 (Figure 2C). C-score is a confidence score for estimating the quality of predicted models, and TM-score is a scale for measuring the structural similarity between two structures by I-TASSER [41]. Subsequently, biological annotations of the predicted PCP protein by COFACTOR and COACH programmes were performed based on the I-TASSER structure prediction. COFACTOR and COACH determine protein functions (ligand-binding sites, EC and GO) using structure comparison and protein-protein networks [42]. As suggested by COFACTOR, the PCP protein was predicted to belong to the biological process (protein-chromophore linkage—GO:0018298) and cellular component (light-harvesting complex—GO: 0030076). COACH predicted 19 ligand binding sites in the predicted PCP protein sequence with peridinin (PID) as major ligand with C-score 0.51 and cluster size 30 (Figure 2D).

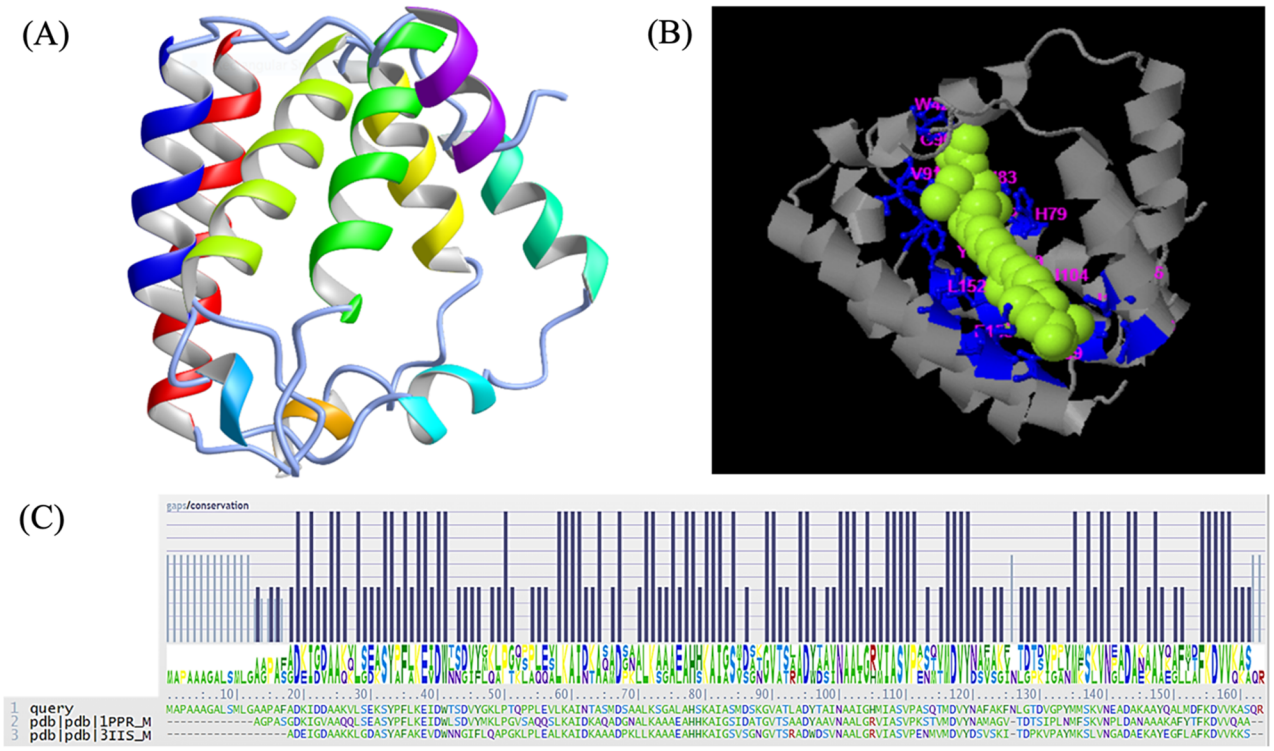

Rank	C-score	Cluster size	PDB Hit	Lig Name	Download Complex	Ligand Binding Site Residues
1	0.51	30	2x1zM	PID	Rep, Mult	42,79,82,83,86,90,91,92,97,100,101,104,108,113,116,152,155,156,159
2	0.24	14	2x1zM	PID	Rep, Mult	36,40,42,47,48,133,134,136,137,145,146,149
3	0.17	15	2x20M	PID	Rep, Mult	46,47,49,50,131,132,135,136
4	0.14	17	2x20M	PID	Rep, Mult	65,66,72,116,117,119,120,153,156
5	0.11	7	3iiuM	J7Z	Rep, Mult	62,65,119,120,123,124,132,133,146,149,150,153

Figure 2. Secondary structure prediction of identified PCP protein sequence matched to accession SimA3.s6014_g3 (**A**), 3D model with ligand binding sites depicted by I-TASSER and COACH (**B**), I-TASSER-based PCP protein (from *S. tridacnidorum*) sequence alignment to template IpprM with highest matching scores (**C**), ligand binding site residues prediction in PCP protein (from *S. tridacnidorum*) sequence by COACH considering 1 pprM as a template model (https://www.rcsb.org/structure/1ppr, accessed on 26 January 2021) (**D**). PID denotes peridinin.

3.3. Spectroscopic Properties of PCP

The absorption spectrum of PCP measured at room temperature (Figure 3A) consisted of a broad band between 400–540 nm with major peaks at 442, 484 and 674 nm. These spectral peaks were assigned to be of Chl *a* Soret band (at 422 nm), broad peridinin band (at 484 nm) and a Chl *a* Qy band (at 674 nm). These peaks were in close proximity to PCP from *Symbiodinium* species and *A. carterae* [12,13,26], with a slight shift of 4 nm for Chl *a*; 8 nm for peridinin and a 4 nm for Chl *a* Qy band. Furthermore, the maximum fluorescence emission (Figure 3B) of purified PCP differed slightly to that of the previously studied species of Symbiodiniaceae [12] with a peak maximum at 676 nm and a vibronic peak at 735 nm.

The observed variations in both absorption and emission spectrum in the present study could be explained on the basis of amino acids sequence analysis. In this study, the predicted PCP sequence was best modelled with *A. carterae* PCP (PDB ID: 2X1Z_M; IpprM) (Figure 2B,C) as supported by COACH and I-TASSER prediction tools. These prediction models suggested a region at 100–108 amino acid sequences, among other regions, as possible peridinin binding sites. It was previously evident that Chl *a* binding sites in the PCP amino acid sequence for both *Symbiodinium* sp. and *A. carterae* lie in the region LKAAAEAHHKAIGSIDA, in which Histidine interacts with Chl *a* through a water

molecule [43] and peridinin binding remains in region VNAALGR. Both these regions matched well (>95% amino acids match) in *Symbiodinium* sp. and *A. carterae* [12]; however, they varied significantly in the *S. tridacnidorum* studied in the present study (Figure 3C). These and other differences in the sequences (responsible for putative Chl *a* and peridinin-binding) could possibly explain the observed differences in absorption and emmision spectrum of PCP in *S. tridacnidorum* when compared to other species of Symbiodiniaceae.

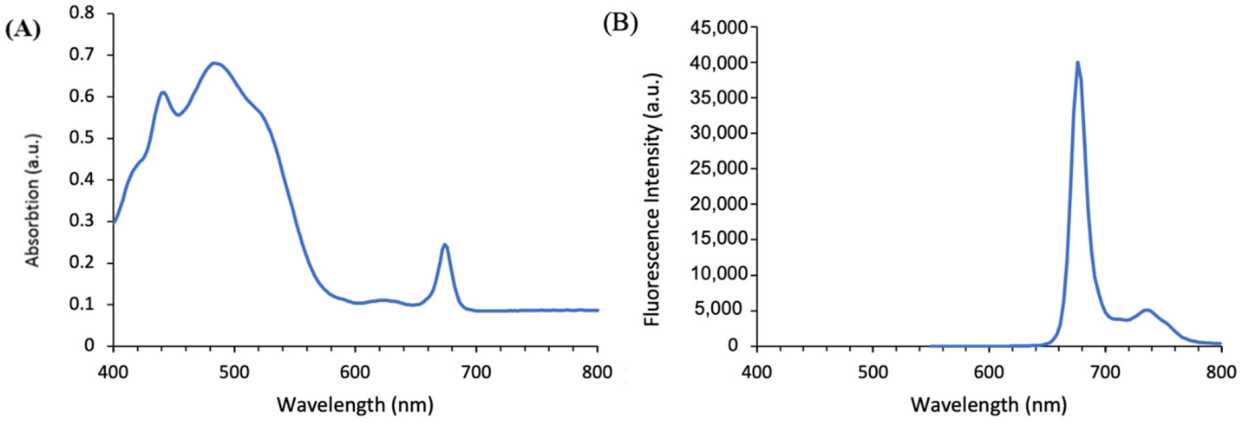

(C)

```
Query   19   ADKIDDAAKVLSEKSYPFLKEIDWTSDVY----GKLPTQPPLEVLKAINT-----ASMDS  69
             AD I DAAK L + SY F KE+DW   ++    GKL    PLE LKAI+      A  D
Sbjct   1    ADEIGDAAKKLGDASYAFAKEVDWNNGIFLQAPGKLQ---PLEALKAIDKMIVMGAAADP  57

Query   70   AALKSGALAHSKAIASM-DSKGVATLADYTAINAAIGHMIASVPASQTMDVYNAFAKFNL  128
               LK  A AH KAI S     GV   AD   +NAA G  IASVP    MDVY+   K
Sbjct   58   KLLKAAAEAHHKAIGSVSGPNGVTSRADWDSVNAALGRVIASVPENMVMDVYDSVSKIT-  116

Query   129  GTDVGPYMMSKVNEADAKAAYQALMDFKDVVKASQ  163
                V  YM S VN ADA  AY+  + FKDVVK SQ
Sbjct   117  DPKVPAYMKSLVNGADAEKAYEGFLAFKDVVKKSQ  151
```

Figure 3. The absorption (**A**) and fluorescence emission (**B**) spectrum of PCP from *S. tridacnidorum*. Predicted PCP protein sequence alignment of *S. tridacnidorum* (query) and *A. carterae (subject)* (**C**). Query sequence matched to subject protein sequence with score 110 bits, expected value 3×10^{-25}, identity (73/155; 47%) and gaps (1/155; 9%). The solid lined peptide sequence is a possible Chl *a* binding site and dotted lined sequence is a possible peridinin-binding site in *S. tridacnidorum* (query) and *A. carterae (subject)*.

3.4. Antioxidant, Anti-Tumour and Anti-Inflamation Bioactivities of PCP

3.4.1. Antioxidant Potential of PCP

In the present study, the purified PCP from *S. tridacnidorum* exhibited significant antioxidant activity by inhibiting the radical cation ABTS radical in a dose-dependent manner. The purified PCP scavenged 50% ABTS radicals at IC_{50} value of 50 µM/mL (Figure 4), which is presumed to be primarily associated with peridinin carotenoid present in PCP. However, the referenced ascorbic acid exhibited higher antioxidant activity, with an IC_{50} value of 0.85 µM/mL (Supplementary Figure S5). Peridinin is a unique allenic oxi-carotenoid and highly abundant in dinoflagellates (55% of total carotenoids), which extends the range of absorption for light harvesting. Consistent with earlier reports, peridinin extracted from the marine algae *Gonyaulax polyedra* exhibited singlet oxygen quenching potential, albeit with low potency (5-fold less) than that of β-carotene [44]. Lower quenching potential of peridinin compared to carotene is suggested to be due to less conjugated double bonds present in their chemical structure [45]. Fucoxanthin, a carotenoid with a structure similar to peridinin, has also been reported to be 10-fold less effective than β-carotene in scavenging reactive radicals but exhibited 13-fold higher hydroxyl

radical scavenging activities than that of α-tocopherol [46]. Interestingly, fucoxanthin and similar carotenoids such as peridinin have shown high antioxidant potential under anoxic conditions, whereas other carotenoids, such as β-carotene and lutein, shown little to no quenching activities in such chemical assessment systems [47].

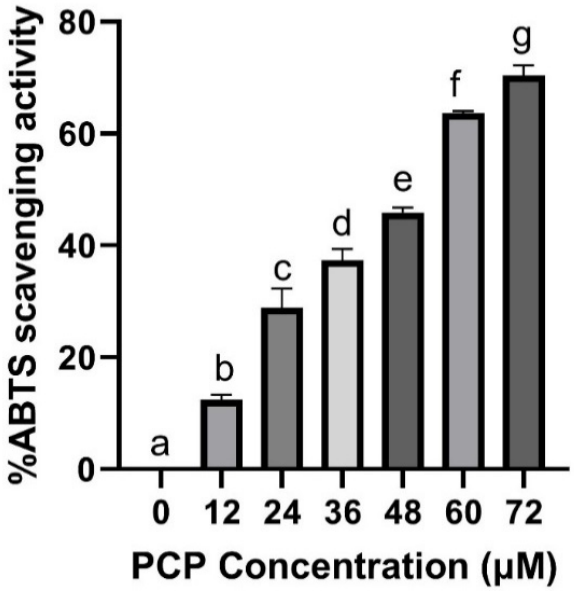

Figure 4. Antioxidant activity of purified PCP on ABTS radical scavenging activity. Results represent the mean ± SD of three replicates. Different superscript letters on column bars denotes significant difference at $p < 0.05$.

Peridinin was found to mitigate atherosclerosis by inhibiting lipid peroxidation in liposomes and primary human endothelial cells [48]. Additionally, chlorophylls of green seaweeds and microalgae have been identified as a rich source of edible antioxidants with strong radical-scavenging activities and reducing power due to pheophorbide content in their structure [8]. Consequently, the inclusion of chlorophyll and carotenoid-based formulations (sourced from micro and macroalgae) in human diets has emerged recently to promote a healthy lifestyle [8]. Therefore, algal PCP enriched in peridinin, and chlorophyll could possibly be considered a promising antioxidant and anti-lipoperoxidant and may serve as an effective biological probe and/or therapeutic.

3.4.2. Anti-Tumour and Anti-Inflammation Potential of PCP from *S. tridacnidorum*

In this research, for the first time we explored the anti-tumour and anti-inflammation potential of purified PCP extracted from *S. tridacnidorum*. Anti-tumour potential of PCP was examined by assessing the viability of HTC-116, MDA-MD 231 and RAW 264.7 cancerous cell lines. PCP significantly reduced the viability of these cells in a dose-dependent manner (Figure 5A–C). However, its noteworthy that PCP responded differentially to these cancerous/tumour cells and displayed moderate anti-tumour activity. For example, PCP exhibited higher anticancer activity against HTC-116 (IC_{50} value 4.3 μM), when compared to MDA-MD 231 (IC_{50} value 5.4 μM; Figure 5A,B). However, PCP did not significantly reduce the cell viability of RAW 264.7 within the concentration range tested herein (0.75–24 μM/mL; Figure 5C). These results suggest a differential selectivity and bioactivity of PCP toward tested tumour cell lines. As such, the precise molecular mechanisms underlying the anti-tumour action of PCP extracted from *S. tridacnidorum* remains to be clarified. Typically, drug candidates require biological activities or IC_{50} values within the nM or μM range, for small organic molecules. For example, the quinazoline derivative gefitinib, an approved cancer chemotherapeutic agent can exert effects with IC_{50} values less than 5 μM for some cells, and closer to 10 μM for other more resistance cell lines (i.e., HTC-116) [49].

Erlotinib, another quinazoline derivative, has also been shown to display IC_{50} values less than 5 µM for some cell lines; however, it has been shown that MDA-MD-231 can be highly resistance with little to no cellular toxicity [50]. Both gefitinib and Erlotinib are low-molecular-weight epidermal growth factor receptor inhibitors of the tyrosine kinase enzymatic activity [51], and it is important to note that the PCP tested herein is classified as a large protein (164 amino acids long). Proteins are not typically defined as ideal drug candidates in molecular nature due to fact that they can be degraded easily and exhibit a short half-life in vivo with potential immunogenicity issues. However, they can exhibit high efficacy and low toxicity with strong specificity and are increasingly attracting interest for drug development [52]. Considering the varied responses of approved drugs across different cell lines, and that proteins can act with strong specificity, it is not surprising that the cellular response to the tested PCP varied herein. As PCP is protein-pigment complex, numerous studies have shown the cytotoxicity potential of carotenoid pigments and have categorized their toxicity as non-toxic (if ≥70% cell viable), weak toxic (50–70%), moderately toxic (30–50%), and highly toxic (≤30%) [53,54]. So far, marine carotenoids including fucoxanthin and its metabolite fucoxanthinol and chlorophyll derivatives have shown considerable potential for prevention and treatment of chronic diseases [10,55].

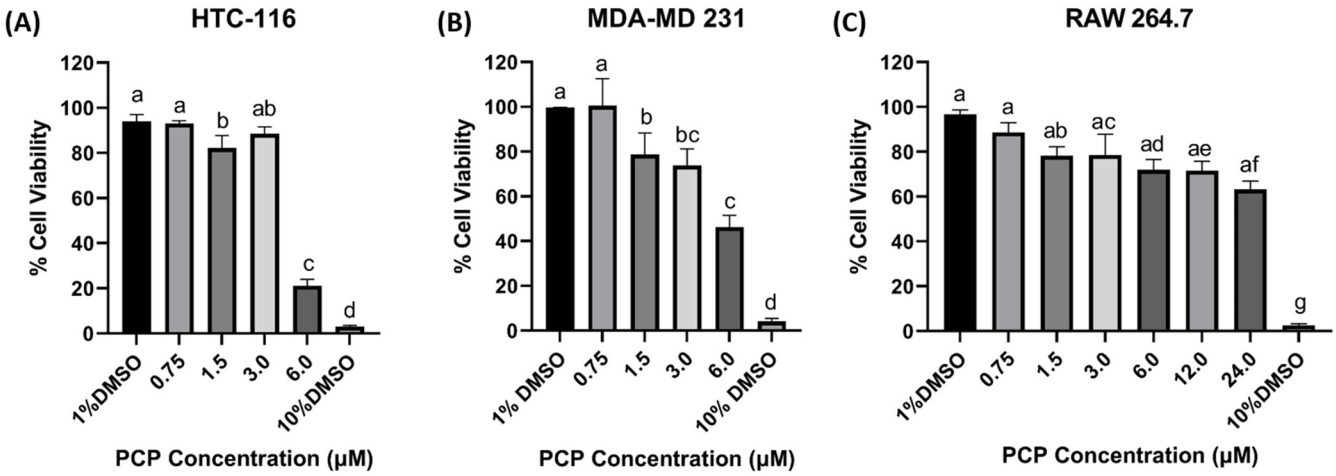

Figure 5. Anti-tumour potential of purified PCP on human colorectal (HTC-116) (**A**), human metastatic breast adenocarcinoma (MDA-MD 231) (**B**), and abelson murine leukaemia virus-induced tumour macrophage (RAW 264.7) (**C**) cancer cell lines. Results represent the mean±SD of three replicates compared to positive control (1% DMSO) and kill control (10% DMSO). Different superscript letters on column bars denotes significant difference at $p < 0.05$.

In support of our findings, [55] demonstrated that peridinin inhibited cell proliferation and viability of HTLV-1-infected T-cell lines by either arresting cells at G1 phase (at 5 µM) or by inducing apoptosis (at 10 µM). Sugawara et al. [10] reported that peridinin (isolated from dinoflagellate *Heterocapsa triquetra*) induced apoptosis in human colorectal cancer cells by activating both caspase-8 and caspase-9. Furthermore, [56] demonstrated fucoxanthin mediated inhibition of leukemic monocyte RAW264 cells by suppression of NF-κB activation and MAPK phosphorylation. Several chlorophyll derivatives (e.g., Chl *a*, pheophytin *a*, pheophytin *b*, pheophorbide *a*) or phycobilins such as phycocyanin have also been shown to reduce viability of cancerous cells [57]. While the precise molecular mechanism for the anti-tumour response of PCP was not explored herein, these findings, along with other reports, suggest PCP (comprised of peridinin and *chl*) could be a potential chemotherapeutic agent; however, how PCP exerts its affects, and its specificity, needs to be further determined.

Furthermore, the anti-inflammatory response of PCP was determined by assessing the inhibition of NO in LPS stimulated macrophages (RAW 264.7). Among the various tested concentrations (Figure 6), PCP at 24 µM significantly reduced NO production (>3 folds) to

10 μM, compared to 35 μM NO produced using 0.75 μM/mL PCP. However, PCP did not significantly reduce NO production at the other tested concentrations (0.75–12 μg/mL). Inhibition of nitric oxide synthase 2 (NOS2), and thereby NO production, or the scavenging of NO, in LPS-stimulated RAW264.7 macrophage cells represent a standard screening system for various anti-inflammatory drugs. With regard to inflammatory activities, potent NO inhibitory activity against lipopolysaccharide (LPS)-induced nitric oxide release will exhibit IC_{50} values up to 10 μM. For example, the L-NG-Monomethyl arginine citrate, a non-selective inhibitor of NOS exhibits an IC_{50} 25.5 μM [58]. In contrast, 3-bromo-7-nitro-1H-indazole is one of the most potent selective inhibitors with 10 μM able to suppress neuronal nitric oxide synthases (NOS-I) activity by 96%, respectively [59]. Onodera et al. [11] suggested peridinin to be a potential agent for suppressing allergic inflammatory responses by inhibiting eosinophil cells in mice. Furthermore, high anti-inflammation potential of various carotenoids including β-carotene, lycopene and fucoxanthin have been documented earlier in reducing the level of pro-inflammatory mediators such as NO, interleukin-1β/6 and tuber necrosis factor (TNF-α) in leukemic monocyte RAW264 cells via inhibition of NF-κB activation and MAPK phosphorylation [56,60,61]. An interesting observation made in this study that PCP inhibits NO production only at higher concentrations (400 μg/mL), which could possibly be due to chlorophyll masked peridinin in the PCP complex, thereby not allowing its interaction directly with inflammatory mediators. Despite this, the presence of biological activities such as antioxidant, antitumor, and anti-inflammation for the PCP extracted and isolated from *Symbiodinium tridacnidorum* as demonstrated in this study suggest a potential for use in the pharmaceutical industry to treat various chronic diseases, thus warranting further investigation.

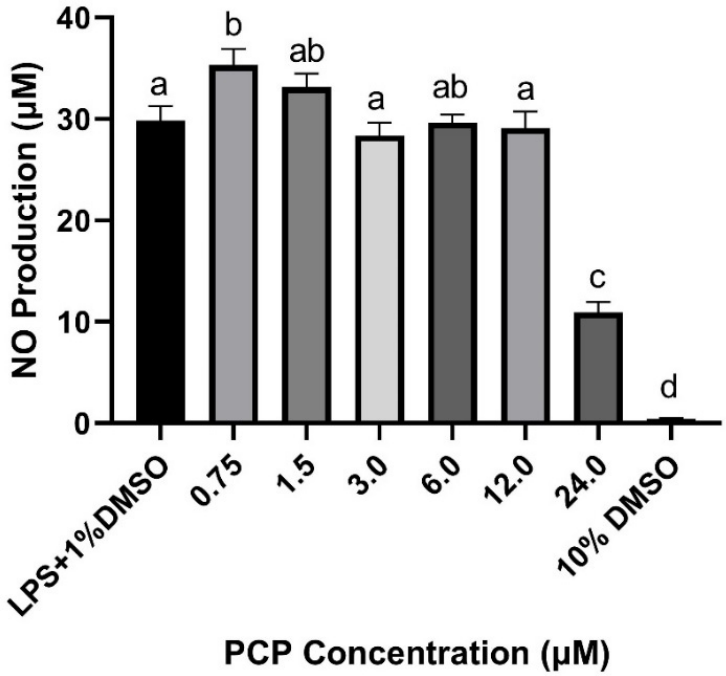

Figure 6. Anti-inflammation potential of purified PCP on lipopolysaccharide (LPS) stimulated NO production in RAW 264.7 macrophage cells. Results represent the mean ± SD of three replicates. Different superscript letters on column bars denotes significant difference at $p < 0.05$.

4. Conclusions

This is the first report of the extraction, purification, characterisation, and bioactivity evaluation of PCP against cancerous cells in terms of antioxidant, antitumor, and anti-inflammatory activities. The AKTA pure system purified intact PCP from *S. tridacnidorum* (CS-73) of molecular weight 17.3 kDa, and 164 amino acids that exhibited several protein binding regions, but no DNA/RNA binding site supports its suitability in designing

diverse protein-conjugates for biomedical application. Moreover, the alanine-rich hydrophobic h-region in the PCP signal peptide sequence confirmed its localisation within thylakoids. Predictprotein COACH and I-TASER tools further predicted the PCP sequence of *S. tridacnidorum* (CS-73) that match closely with *A. carterae* PCP, with a slight variation in *chl* and peridinin binding regions. These variations possibly explained the shift in PCP absorption and emission spectra compared to other *Symbiodinium* sp. Interestingly, PCP, with IC50 values between 4–20 µM, exhibited significant anti-tumour and anti-inflammatory properties (against HTC-116 and MDA-MD 231 cancerous cell lines), indicating that it is not only a photoprotective and light harvester protein, but a novel bioactive compound for pharmaceutical industry use. It is, however, noteworthy that PCP displayed low bioactivity against RAW 264.7, and is therefore warranted to explore the molecular mechanism of PCP bioactivity. The stability of the molecule should be examined further, either as a free molecule or embedded as part of emulsions and encapsulations for its use in pharmaceuticals and cosmetic industries. Such futuristic studies can speed up the progress towards its commercialisation and incorporation of PCP in the global market.

Supplementary Materials: The following are available online at https://www.mdpi.com/article/10.3390/jmse9121387/s1. Figure S1: *Symbiodinium tridacnidorum* (ITS2-type A3, CS73) cultures in incubator and purified PCP (orange solution) using ÄKTA™ PURE system. Figure S2: Protein sequence similarity of purified PCP *from Symbiodinium tridacnidorum* using Peaks Studio 8.5 (A). Total matched peptides (blue), unique peptides (*), and sequence coverage (shaded black and green amino acid regions) identified in MS analysis after trypsin digestion of PCP (B). Subscript letters (o, d) on identified peptides denotes oxidation and deamination post-translational modifications (PTMs). Figure S3. Signal peptide (SP) sequence in PCP protein purified from *S. tridacnidorum* (based on amino acid sequence inferred from accession SimA3.s6014_g3) flank in first 19 amino acids confirmed by Phobius software (A). SP (encircled section) consist of three regions namely C (cleavage region recognition by signal peptidase-orange), N (hydrophilic and a positively charged region-green) and H (central hydrophobic region-red). Alanine rich region (in central hydrophobic H region) 4–14 amino acids of signal peptide (B). Figure S4. Predict Protein bioinformatic tools depict secondary structures information (A,B), solvent accessibility (A,C), topology (A,D) and protein binding features (A) based on predicted PCP protein sequence of *S. tridacnidorum*. Figure S5. ABTS scavenging activity of reference standard ascorbic acid with IC50 value 0.85 µM/mL.

Author Contributions: Conceptualisation and the experimental design, K.M.S., M.K., J.I.M., A.S. and P.J.R.; methodology, K.M.S., M.K., J.I.M. and A.S.; contributed to proteomic analysis, M.K., M.P.P. and K.M.S.; data collection, K.M.S., J.I.M., A.S. and M.K. and data analysis, M.K., J.I.M. and K.M.S.; supervision, P.J.R. and M.K.; writing—original draft preparation, K.M.S. and M.K.; writing—review and editing, M.K., K.M.S., P.J.R., J.I.M., A.S., A.H. and T.O. All authors have read and agreed to the published version of the manuscript.

Funding: This work was funded by ARC linkage grant (LP150100751) to P.J.R. and UTS IRS Scholarship to K.M.S.

Institutional Review Board Statement: Not applicable.

Informed Consent Statement: Not applicable.

Data Availability Statement: The supplementary files reported can also be found at https://zenodo.org/deposit/5760130 (accessed on 24 January 2021).

Acknowledgments: The authors would like to thank T.O. and AKTA specialists for their help with operating the AKTA purification system and UTS proteomics core facility for nano-LC-MS/MS.

Conflicts of Interest: The authors declare no conflict of interest.

References

1. Carbonera, D.; Di Valentin, M.; Spezia, R.; Mezzetti, A. The unique photophysical properties of the Peridinin-Chlorophyll-a-Protein. *Curr. Protein Pept. Sci.* **2014**, *15*, 332–350. [CrossRef] [PubMed]
2. Mirkovic, T.; Ostroumov, E.E.; Anna, J.M.; Van Grondelle, R.; Scholes, G.D. Light absorption and energy transfer in the antenna complexes of photosynthetic organisms. *Chem. Rev.* **2017**, *117*, 249–293. [CrossRef] [PubMed]

3. Takahashi, S.; Whitney, S.; Itoh, S.; Maruyama, T.; Badger, M. Heat stress causes inhibition of the de novo synthesis of antenna proteins and photobleaching in cultured *Symbiodinium*. *Proc. Natl. Acad. Sci. USA* **2008**, *105*, 4203–4208. [CrossRef] [PubMed]
4. Mackowski, S. Metallic nanoparticles coupled with photosynthetic complexes. *Smart Nanoparticles Technol.* **2012**, *2012*, 3–28.
5. Niedziółka-Jönsson, J.; Mackowski, S. Plasmonics with Metallic Nanowires. *Materials* **2019**, *12*, 1418. [CrossRef] [PubMed]
6. Szalkowski, M.; Sulowska, K.; Grzelak, J.; Niedziółka-Jönsson, J.; Roźniecka, E.; Kowalska, D.; Mackowski, S. Wide-Field fluorescence microscopy of real-time bioconjugation Sensing. *Sensors* **2018**, *18*, 290. [CrossRef] [PubMed]
7. Li, T.; Ding, T.; Li, J. Medicinal purposes: Bioactive metabolites from marine-derived organisms. *Mini Rev. Med. Chem.* **2019**, *19*, 138–164. [CrossRef]
8. Pérez-Gálvez, A.; Viera, I.; Roca, M. Carotenoids and chlorophylls as antioxidants. *Antioxidants* **2020**, *9*, 505. [CrossRef]
9. Torregrosa-Crespo, J.; Montero, Z.; Fuentes, J.L.; García-Galbis, M.R.; Garbayo, I.; Vílchez, C.; Martínez-Espinosa, R.M. Exploring the valuable carotenoids for the large-scale production by marine microorganisms. *Mar. Drugs* **2018**, *16*, 203. [CrossRef]
10. Sugawara, T.; Yamashita, K.; Sakai, S.; Asai, A.; Nagao, A.; Shiraishi, T.; Imai, I.; Hirata, T. Induction of apoptosis in DLD-1 human colon cancer cells by peridinin isolated from the dinoflagellate, *Heterocapsa triquetra*. *Biosci. Biotechnol. Biochem.* **2007**, *71*, 1069–1072. [CrossRef]
11. Onodera, K.-I.; Konishi, Y.; Taguchi, T.; Kiyoto, S.; Tominaga, A. Peridinin from the marine symbiotic dinoflagellate, *Symbiodinium* sp., regulates eosinophilia in mice. *Mar. Drugs* **2014**, *12*, 1773–1787. [CrossRef]
12. Jiang, J.; Zhang, H.; Kang, Y.; Bina, D.; Lo, C.S.; Blankenship, R.E. Characterization of the peridinin-chlorophyll a-protein complex in the dinoflagellate *Symbiodinium*. *Biochim. Biophys. Acta* **2012**, *1817*, 983–989. [CrossRef]
13. Jiang, J.; Zhang, H.; Orf, G.S.; Lu, Y.; Xu, W.; Harrington, L.B.; Liu, H.; Lo, C.S.; Blankenship, R.E. Evidence of functional trimeric chlorophyll a/c2-peridinin proteins in the dinoflagellate *Symbiodinium*. *Biochim. Biophys. Acta Bioenerg.* **2014**, *1837*, 1904–1912. [CrossRef] [PubMed]
14. Miller, D.J.; Catmull, J.; Puskeiler, R.; Tweedale, H.; Sharples, F.P.; Hiller, R.G. Reconstitution of the peridinin–chlorophyll a protein (PCP): Evidence for functional flexibility in chlorophyll binding. *Photosynth. Res.* **2005**, *86*, 229–240. [CrossRef]
15. Weis, V.M.; Verde, E.A.; Reynolds, W.S. Characterization of a short form peridinin-chlorophyll-protein (PCP) cDNA and protein from the symbiotic dinoflagellate *Symbiodinium muscatinei* (Dinophyceae) from the sea anemone *Anthopleura elegantissima* (Cnidaria). *J. Phycol.* **2002**, *38*, 157–163. [CrossRef]
16. Wörmke, S.; Mackowski, S.; Schaller, A.; Brotosudarmo, T.H.; Johanning, S.; Scheer, H.; Bräuchle, C. Single molecule fluorescence of native and refolded peridinin–chlorophyll–protein complexes. *J. Flu* **2008**, *18*, 611–617. [CrossRef]
17. Supasri, K.; Kumar, M.; Mathew, M.; Signal, B.; Padula, M.; Suggett, D.; Ralph, P. Evaluation of filter, paramagnetic, and STAGETips aided workflows for proteome profiling of Symbiodiniaceae dinoflagellate. *Processes* **2021**, *9*, 983. [CrossRef]
18. Ogata, T.; Kodama, M.; Nomura, S.; Kobayashi, M.; Nozawa, T.; Katoh, T.; Mimuro, M. A novel peridinin—Chlorophyll a protein (PCP) from the marine dinoflagellate *Alexandrium cohorticula*: A high pigment content and plural spectral forms of peridinin and chlorophyll *a*. *FEBS Lett.* **1994**, *356*, 367–371. [CrossRef]
19. Yu, L.; Li, T.; Li, L.; Lin, X.; Li, H.; Liu, C.; Guo, C.; Lin, S. SAGER: A database of Symbiodiniaceae and Algal Genomic Resource. *Database* **2020**, *2020*. [CrossRef]
20. Re, R.; Pellegrini, N.; Proteggente, A.; Pannala, A.; Yang, M.; Rice-Evans, C. Antioxidant activity applying an improved ABTS radical cation decolorization assay. *Free Radic. Biol. Med.* **1999**, *26*, 1231–1237. [CrossRef]
21. McCauley, J.; Zivanovic, A.; Skropeta, D. Bioassays for Anticancer Activities. In *Metabolomics Tools for Natural Product Discovery*; Springer: Berlin/Heidelberg, Germany, 2013; pp. 191–205.
22. McCauley, J.I.; Meyer, B.J.; Winberg, P.C.; Ranson, M.; Skropeta, D. Selecting Australian marine macroalgae based on the fatty acid composition and anti-inflammatory activity. *J. Appl. Phycol.* **2015**, *27*, 2111–2121. [CrossRef]
23. Takahashi, S.; Yoshida, M.; Watanabe, M.M.; Isoda, H. Anti-Inflammatory effects of *Aurantiochytrium limacinum* 4W-1b ethanol extract on murine macrophage RAW264 Cells. *BioMed Res. Int.* **2019**, *2019*, 3104057. [CrossRef]
24. Hofmann, E.; Wrench, P.M.; Sharples, F.P.; Hiller, R.G.; Welte, W.; Diederichs, K. Structural basis of light harvesting by carotenoids: Peridinin-chlorophyll-protein from *Amphidinium carterae*. *Science* **1996**, *272*, 1788–1791. [CrossRef]
25. Hiller, R.; Crossley, L.; Wrench, P.; Santucci, N.; Hofmann, E. The 15-kDa forms of the apo-peridinin-chlorophyll a protein (PCP) in dinoflagellates show high identity with the apo-32 kDa PCP forms, and have similar N-terminal leaders and gene arrangements. *Mol. Genet. Genom* **2001**, *266*, 254–259. [CrossRef]
26. Iglesias-Prieto, R.; Govind, N.; Trench, R. Apoprotein composition and spectroscopic characterization of the water-soluble peridinin—Chlorophyll a—Proteins from three symbiotic dinoflagellates. *Proc. R. Soc. B.* **1991**, *246*, 275–283.
27. Haxo, F.T.; Kycia, J.H.; Somers, G.F.; Bennett, A.; Siegelman, H.W. Peridinin-chlorophyll a proteins of the dinoflagellate *Amphidinium carterae* (Plymouth 450). *Plant. Physiol.* **1976**, *57*, 297–303. [CrossRef]
28. Reichman, J.R.; Wilcox, T.P.; Vize, P.D. PCP gene family in *Symbiodinium* from *Hippopus hippopus*: Low levels of concerted evolution, isoform diversity, and spectral tuning of chromophores. *Mol. Biol. Evol.* **2003**, *20*, 2143–2154. [CrossRef] [PubMed]
29. Trench, R.K.; Blank, R.J. *Symbiodinium Microadriaticum* Freudenthal, *S. goreauii* Sp. Nov., *S. kawagutii* Sp. Nov. and *S. pilosum* Sp. Nov.: *Gymnodinioid* Dinoflagellate symbionts of marine invertebrates. *J. Phycol.* **1987**, *23*, 469–481. [CrossRef]
30. Chang, S.S.; Trench, R. Peridinin—Chlorophyll a proteins from the symbiotic dinoflagellate *Symbiodinium* (=*Gymnodinium*) *microadriaticum*, Freudenthal. *Proc. R. Soc. B.* **1982**, *215*, 191–210.

31. Prézelin, B.B.; Haxo, F.T. Purification and characterization of peridinin-chlorophyll a-proteins from the marine dinoflagellates *Glenodinium* sp. and *Gonyaulax polyedra*. *Planta* **1976**, *128*, 133–141. [CrossRef] [PubMed]
32. Shoguchi, E.; Beedessee, G.; Tada, I.; Hisata, K.; Kawashima, T.; Takeuchi, T.; Arakaki, N.; Fujie, M.; Koyanagi, R.; Roy, M.C.; et al. Two divergent *Symbiodinium* genomes reveal conservation of a gene cluster for sunscreen biosynthesis and recently lost genes. *BMC Genom.* **2018**, *19*, 458. [CrossRef] [PubMed]
33. Boldt, L.; Yellowlees, D.; Leggat, W. Hyperdiversity of genes encoding integral light-harvesting proteins in the dinoflagellate *Symbiodinium* sp. *PLoS ONE* **2012**, *7*, e47456. [CrossRef]
34. Stomp, M.; Huisman, J.; Stal, L.J.; Matthijs, H.C. Colorful niches of phototrophic microorganisms shaped by vibrations of the water molecule. *ISME J.* **2007**, *1*, 271–282. [CrossRef] [PubMed]
35. Balsera, M.; Soll, J.; Bölter, B. Protein import machineries in endosymbiotic organelles. *Cell. Mol. Life Sci.* **2009**, *66*, 1903–1923. [CrossRef] [PubMed]
36. Le, Q.; Markovic, P.; Hastings, J.; Jovine, R.; Morse, D. Structure and organization of the peridinin-chlorophyll a-binding protein gene in *Gonyaulax polyedra*. *Mol. Gen. Genet.* **1997**, *255*, 595–604. [CrossRef] [PubMed]
37. Ludington, J.L. Protein Binding Site Analysis for drug Discovery Using a Computational Fragment-Based Method. In *Fragment-Based Methods in Drug Discovery*; Springer: Berlin/Heidelberg, Germany, 2015; pp. 145–154.
38. Kozlowski, L.P.; Bujnicki, J.M. MetaDisorder: A meta-server for the prediction of intrinsic disorder in proteins. *BMC Bioinform.* **2012**, *13*, 111. [CrossRef]
39. Breuza, L.; Poux, S.; Estreicher, A.; Famiglietti, M.L.; Magrane, M.; Tognolli, M.; Bridge, A.; Baratin, D.; Redaschi, N. The UniProtKB guide to the human proteome. *Database* **2016**, *2016*. [CrossRef]
40. Dray, E.L.; Ousley, C.G.; McKim, D.B. Methodological considerations for the enrichment of bone marrow endothelial and mesenchymal stromal cells. *Mol. Immunol.* **2021**, *131*, 127–136. [CrossRef]
41. Yang, J.; Zhang, Y. I-TASSER server: New development for protein structure and function predictions. *Nucleic Acids Res.* **2015**, *43*, W174–W181. [CrossRef]
42. Zhang, C.; Freddolino, P.L.; Zhang, Y. COFACTOR: Improved protein function prediction by combining structure, sequence and protein–protein interaction information. *Nucleic Acids Res.* **2017**, *45*, W291–W299. [CrossRef] [PubMed]
43. Schulte, T.; Hiller, R.G.; Hofmann, E. X-ray structures of the peridinin–chlorophyll-protein reconstituted with different chlorophylls. *FEBS Lett.* **2010**, *584*, 973–978. [CrossRef]
44. Pinto, E.; Catalani, L.H.; Lopes, N.P.; Di Mascio, P.; Colepicolo, P. Peridinin as the major biological carotenoid quencher of singlet oxygen in marine algae *Gonyaulax polyedra*. *Biochem. Biophys. Res. Commun.* **2000**, *268*, 496–500. [CrossRef] [PubMed]
45. Foote, C.S.; Denny, R.; Weaver, L.; Chang, D.Y.; Peters, J. Quenching of singlet oxygen. *Ann. N. Y. Acad. Sci.* **1970**, *171*, 139–148. [CrossRef]
46. Sachindra, N.M.; Sato, E.; Maeda, H.; Hosokawa, M.; Niwano, Y.; Kohno, M.; Miyashita, K. Radical scavenging and singlet oxygen quenching activity of marine carotenoid fucoxanthin and its metabolites. *J. Agric. Food Chem.* **2007**, *55*, 8516–8522. [CrossRef] [PubMed]
47. Nomura, T.; Kikuchi, M.; Kubodera, A.; Kawakami, Y. Proton-donative antioxidant activity of fucoxanthin with 1, 1-diphenyl-2-picrylhydrazyl (DPPH). *IUBMB Life* **1997**, *42*, 361–370. [CrossRef]
48. Haley, H.M.; Hill, A.G.; Greenwood, A.I.; Woerly, E.M.; Rienstra, C.M.; Burke, M.D. Peridinin is an exceptionally potent and membrane-embedded inhibitor of bilayer lipid peroxidation. *J. Am. Chem. Soc.* **2018**, *140*, 15227–15240. [CrossRef] [PubMed]
49. Feng, Y.-H.; Tsao, C.-J.; Wu, C.-L.; Chang, J.-G.; Lu, P.-J.; Yeh, K.-T.; Shieh, G.-S.; Shiau, A.-L.; Lee, J.-C. Sprouty2 protein enhances the response to gefitinib through epidermal growth factor receptor in colon cancer cells. *Cancer Sci.* **2010**, *101*, 2033–2038. [CrossRef] [PubMed]
50. Yamasaki, F.; Zhang, D.; Bartholomeusz, C.; Sudo, T.; Hortobagyi, G.N.; Kurisu, K.; Ueno, N.T. Sensitivity of breast cancer cells to erlotinib depends on cyclin-dependent kinase 2 activity. *Mol. Cancer. Ther.* **2007**, *6*, 2168–2177. [CrossRef]
51. Cascone, T.; Morelli, M.; Ciardiello, F. Small molecule epidermal growth factor receptor (EGFR) tyrosine kinase inhibitors in non-small cell lung cancer. *Ann. Oncol.* **2006**, *17*, ii46–ii48. [CrossRef]
52. Cao, S.-J.; Lv, Z.-Q.; Guo, S.; Jiang, G.-P.; Liu, H.-L. An Update-Prolonging the action of protein and peptide drugs. *J. Drug Deliv. Sci. Technol.* **2021**, *61*, 102124. [CrossRef]
53. Araújo, L.C.C.; Aguiar, J.; Napoleão, T.; Mota, F.V.B.; Barros, A.L.S.; Moura, M.C.; Coriolano, M.C.; Coelho, L.C.B.B.; Silva, T.G.; Paiva, P. Evaluation of cytotoxic and anti-inflammatory activities of extracts and lectins from *Moringa oleifera* seeds. *PLoS ONE* **2013**, *8*, e81973. [CrossRef]
54. Mashjoor, S.; Yousefzadi, M.; Esmaeili, M.A.; Rafiee, R. Cytotoxicity and antimicrobial activity of marine macroalgae (Dictyotaceae and Ulvaceae) from the Persian Gulf. *Cytotechnology* **2016**, *68*, 1717–1726. [CrossRef] [PubMed]
55. Ishikawa, C.; Jomori, T.; Tanaka, J.; Senba, M.; Mori, N. Peridinin, a carotenoid, inhibits proliferation and survival of HTLV-1-infected T-cell lines. *Int. J. Oncol.* **2016**, *49*, 1713–1721. [CrossRef]
56. Kim, K.N.; Heo, S.J.; Yoon, W.J.; Kang, S.M.; Ahn, G.; Yi, T.H.; Jeon, Y.J. Fucoxanthin inhibits the inflammatory response by suppressing the activation of NF-κB and MAPKs in lipopolysaccharide-induced RAW 264.7 macrophages. *Eur. J. Pharmacol.* **2010**, *649*, 369–375. [CrossRef] [PubMed]
57. Guerin, M.; Huntley, M.E.; Olaizola, M. Haematococcus astaxanthin: Applications for human health and nutrition. *Trends Biotechnol.* **2003**, *21*, 210–216. [CrossRef]

58. Cheenpracha, S.; Park, E.-J.; Rostama, B.; Pezzuto, J.M.; Chang, L.C. Inhibition of nitric oxide (NO) production in lipopolysaccharide (LPS)-activated murine macrophage RAW 264.7 cells by the norsesterterpene peroxide, epimuqubilin A. *Mar. Drugs* **2010**, *8*, 429–437. [CrossRef] [PubMed]
59. Claramunt, R.M.; López, C.; Pérez-Medina, C.; Pérez-Torralba, M.; Elguero, J.; Escames, G.; Acuña-Castroviejo, D. Fluorinated indazoles as novel selective inhibitors of nitric oxide synthase (NOS): Synthesis and biological evaluation. *Bioorganic Med. Chem.* **2009**, *17*, 6180–6187. [CrossRef]
60. Heo, S.-J.; Yoon, W.-J.; Kim, K.-N.; Ahn, G.-N.; Kang, S.-M.; Kang, D.-H.; Affan, A.; Oh, C.; Jung, W.-K.; Jeon, Y.-J. Evaluation of anti-inflammatory effect of fucoxanthin isolated from brown algae in lipopolysaccharide-stimulated RAW 264.7 macrophages. *Food. Chem. Toxicol.* **2010**, *48*, 2045–2051. [CrossRef]
61. Su, J.; Guo, K.; Huang, M.; Liu, Y.; Zhang, J.; Sun, L.; Li, D.; Pang, K.-L.; Wang, G.; Chen, L.; et al. Fucoxanthin, a Marine Xanthophyll Isolated From *Conticribra weissflogii* ND-8: Preventive Anti-Inflammatory Effect in a Mouse Model of Sepsis. *Front. Pharmacol.* **2019**, *10*, 906. [CrossRef]